

# Isomerization Dynamics of Photochromic Spiropyran Molecular Switches in Phospholipid Bilayers

Christopher J. Wohl and Darius Kuciauskas\*

Department of Chemistry, Virginia Commonwealth University, 1001 West Main Street,  
Richmond, Virginia 23284-2006

Received: July 14, 2005; In Final Form: September 22, 2005

Transient absorption spectroscopy was used to investigate the dynamics of the photochromic indolinobenzo-spiropyran reaction in toluene solution and in phosphatidylcholine bilayers (1,2-dimyristoyl-*sn*-glycero-3-phosphocholine (DMPC), 1,2-dipalmitoyl-*sn*-glycero-3-phosphocholine (DPPC), and 1,2-dioleoyl-*sn*-glycero-3-phosphocholine (DOPC)). After excitation with UV light, colorless (*R/S*)-2-(3',3'-dimethyl-6-nitro-3'H-spiro[chromene-2,2'-indol]-1'-yl)ethanol derivatives are converted to colored merocyanine products in high yield;  $\Phi = 0.45$  in DMPC liposomes. We find that the reaction occurs in the bilayer aliphatic region in the gel ( $P_{\beta'}$ ) and liquid ( $L_{\alpha}$ ) phases. The Arrhenius activation energy for the isomerization in DMPC bilayers was  $\sim 3.5$  times larger in the liquid phase ( $L_{\alpha}$ ,  $E_a = 26.0 \pm 1.0$  kJ mol $^{-1}$ ) than that in the gel phase ( $P_{\beta'}$ ,  $E_a = 7.3 \pm 1.6$  kJ mol $^{-1}$ ). Analysis of the isomerization rate constant temperature dependence allows an estimation of the bilayer viscosity and free volume properties in the  $L_{\alpha}$  phase.

## Introduction

Phospholipid bilayer aggregates, such as liposomes, are commonly used as cell membrane models. The physical properties of phospholipid bilayers are often derived from spectroscopic studies conducted on membrane-embedded molecular sensitizers.<sup>1</sup> Fluorescent membrane probes with large solvatochromic shifts are often used; however, different molecular probes and experimental approaches are needed to study a wider range of bilayer properties. One such approach is the study of excited-state reactions in phospholipid bilayers.<sup>2</sup>

We investigated the spiropyran/merocyanine photochemical reaction in phospholipid bilayers (Scheme 1). (*R/S*)-2-(3',3'-Dimethyl-6-nitro-3'H-spiro[chromene-2,2'-indol]-1'-yl)ethanol molecular sensitizers (SP) consist of two orthogonal moieties, substituted indole and benzopyran, weakly interacting in the ground state.<sup>3</sup> The SP molecular structure is similar to that of well-characterized 6-nitrospiro[2H-1-benzopyran-2,2'-indoline] (6-nitroBIPS)<sup>4,5</sup> except that the dimethylindole moiety of SP is substituted with a (CH $_2$ ) $_2$ OH group. Ring-opening at the conical intersection of the excited-state and the ground-state potential energy surfaces results in ultrafast (several hundred femtoseconds) spiropyran C $_{\text{spiro}}$ –O bond cleavage.<sup>4–6</sup> Subsequent isomerization leads to merocyanine (MC) formation. Experimental and theoretical studies were applied to spiropyran photochemical reaction dynamics,<sup>4,5,7–9</sup> excited-state potential energy surfaces,<sup>10</sup> photochemical reaction pathways,<sup>11</sup> and the structural identity of reaction intermediates and products.<sup>12,13</sup> The two merocyanine isomers shown in Scheme 1 have been reported as having the lowest ground-state energies.<sup>12,14</sup> Our earlier analysis of MC excited-state dynamics indicated that at least two isomers are present in toluene solution.<sup>15</sup> One of the unusual features of spiropyran/merocyanine photochemistry is the sensitivity of this reaction to the medium's polarity, rigidity, and free volume; this supports the use of SP/MC reactions in

various applications.<sup>6</sup> The interaction of spiropyran/merocyanine compounds with lipid and surfactant membranes has been studied.<sup>16–18</sup> In particular, the spiropyran/merocyanine photochemical reaction has been used to reversibly control ion transport across the bilayer.<sup>18</sup>

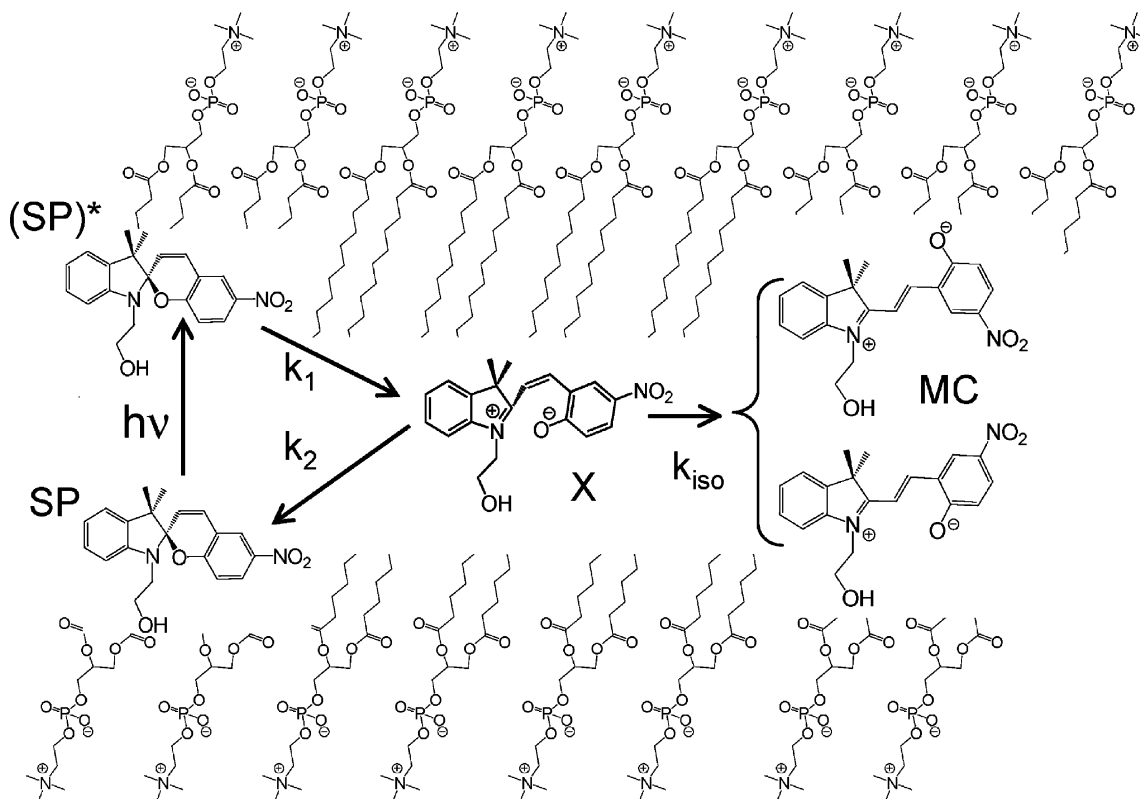
By utilizing the ultrafast SP  $\rightarrow$  MC photochromic reaction and femtosecond pump–probe spectroscopic experiments, we study dynamics in phospholipid bilayers on a picosecond time scale. In particular, we consider phase transitions in phosphatidylcholine bilayers. Phospholipid bilayers exhibit rich polymorphism. In single-component phosphatidylcholine bilayers, the gel ( $L_{\beta'}$  and  $P_{\beta'}$ ) and liquid ( $L_{\alpha}$ ) phases are the most significant, and the  $P_{\beta'} \leftrightarrow L_{\alpha}$  phase transition is considered the most important.<sup>19</sup> Several physical properties are altered during this transition. In particular, the bilayer thickness in the  $P_{\beta'}$  phase is greater by  $\sim 25\%$  than that in the  $L_{\alpha}$  phase.<sup>19</sup> The lipid leaflets are clearly separated in the  $P_{\beta'}$  phase.<sup>19</sup> The conformations of the lipid chains change from a highly ordered all-trans geometry in the  $P_{\beta'}$  phase to a more disordered, liquid-like structure in the  $L_{\alpha}$  phase.<sup>19</sup> The  $L_{\alpha}$  phase best corresponds to the biological membrane state. Theoretical models developed to study reactions in solution have been successfully applied to reactions in phospholipid bilayers.<sup>20</sup>

Below we show that SP  $\rightarrow$  MC isomerization dynamics are sensitive to the structural changes that occur during the  $P_{\beta'} \leftrightarrow L_{\alpha}$  phase transition in phosphatidylcholine bilayers. In the  $L_{\alpha}$  phase, isomerization dynamics are similar to those observed in liquids except that higher viscosities present in phospholipid bilayers reduce the reaction rate. The isomerization rate constants in the bilayer  $L_{\alpha}$  phase are analyzed using Kramers theory, and the results are compared to bilayer free volume properties predicted in simulations.<sup>21–25</sup>

## Experimental Section

**Materials and Methods.** 1,2-Dimyristoyl-*sn*-glycero-3-phosphocholine (DMPC), 1,2-dipalmitoyl-*sn*-glycero-3-phosphocholine (DPPC), and 1,2-dioleoyl-*sn*-glycero-3-phosphocholine

\* Author to whom correspondence should be addressed. Phone: (804) 828-8551. Fax: (804) 828-8599. E-mail: dkuciauskas@vcu.edu.

**SCHEME 1: Spiropyran Photochemical Reaction in Phospholipid Bilayers and Spiropyran (SP)/Merocyanine (MC) Molecular Structures**


(DOPC) lipids were obtained from Avanti Polar Lipids. All other reagents and solvents were obtained from Aldrich. Spiropyran molecular sensitizers ((*R/S*)-2-(3',3'-dimethyl-6-nitro-3'-H-spiro[chromene-2,2'-indol]-1'-yl)ethanol, SP) were synthesized using a literature method<sup>3</sup> and characterized by NMR, elemental analysis, and UV-vis spectroscopy. Absorption spectra were measured with a HP8452A diode array spectrometer.

**Liposome Preparation.** To prepare liposomes, spiropyran and phospholipid solutions were mixed in a round-bottom flask (the phospholipid/spiropyran molar ratio was 50:1), and the organic solvent was removed under an N<sub>2</sub> stream. The flask was placed in a warm-water bath (with the temperature above the phospholipid main phase transition temperature), and the phospholipids were hydrated with a phosphate buffer (50 mM, pH 7) to a final phospholipid concentration of 7.4 mM. This aqueous solution was then agitated with a low power (10 W) ultrasonic bath until homogeneous in appearance and extruded 11 times through a polycarbonate filter (50 nm pore diameter). This preparation yielded single lamellar liposomes with a narrow size distribution and an average liposome diameter of  $75 \pm 2$  nm. Dynamic light scattering with a ZetaSizer from Malvern Instruments was used to determine liposome size.

**Transient Absorption Spectroscopy.** The pump-probe transient absorption spectrometer was described.<sup>15</sup> Laser pulses (325 nm) were used for selective spiropyran excitation (spiropyran absorbance at this wavelength was  $\sim 0.3$ , merocyanine absorbance was  $< 0.1$ ). Excitation pulses (100 fs, 1 kHz) were obtained by frequency-doubling 650 nm optical parametric amplifier (OPA) pulses in a 0.5-mm-thick  $\beta$ -barium borate (BBO) crystal. The energies of the pump and probe pulses were  $\sim 2$  and  $< 1$   $\mu$ J, respectively. To eliminate polarization effects, the relative polarization of the pump and probe beams was set at a "magic angle" (54°). Interference filters (10 nm bandwidth) were used to select the probe wavelength from a white light

continuum generated in a 2-mm-thick sapphire plate. Sample temperature was adjusted with a thermostat to  $\pm 1$  °C. A 1 mm optical path flow cell attached to a peristaltic pump was used. The flow rate was 1.7 mL/min. Changing the laser repetition rate or sample flow rate did not influence the transient absorption signals.

## Results

### SP/MC Transient Absorption Difference Spectra and Kinetics in DMPC Bilayers and in Toluene Solution.

Transient absorption difference spectra of dimyristoylphosphatidylcholine (DMPC) bilayers embedded with SP sensitizers measured after excitation with 325 nm, 100 fs laser pulses are shown in Figure 1. At 0–20 ps time delay, a positive signal at 480–540 nm and a negative signal at 600–650 nm are observed. In earlier ultrafast studies of the related 6-nitroBIPS spiropyran, the positive 480–540 nm signal has been assigned to the cisoidal intermediate X formed after breaking the C<sub>spiro</sub>–O bond (Scheme 1).<sup>4,7</sup> Recently it was suggested that this signal is observed after spiropyran internal conversion.<sup>5</sup> The negative signal at 600–650 nm is attributed to intermediate X and merocyanine MC stimulated emission.<sup>26</sup> (In this wavelength region, MC steady-state fluorescence emission is observed.<sup>15</sup>) To investigate this assignment further, we measured picosecond difference spectra with direct excitation of the MC form (a 380 nm excitation wavelength was used). The negative signal amplitude at 600–650 nm was enhanced with 380 nm excitation, thus confirming the negative signal assignment to stimulated emission.

A strong transient absorption signal with the maximum at  $\sim 580$  nm grows on a picosecond time scale. This photochromic absorption band is assigned to merocyanine.<sup>4,7</sup> At 800 ps (and longer) time delay, the transient absorption spectrum in DMPC bilayers is essentially identical to the MC absorption spectrum

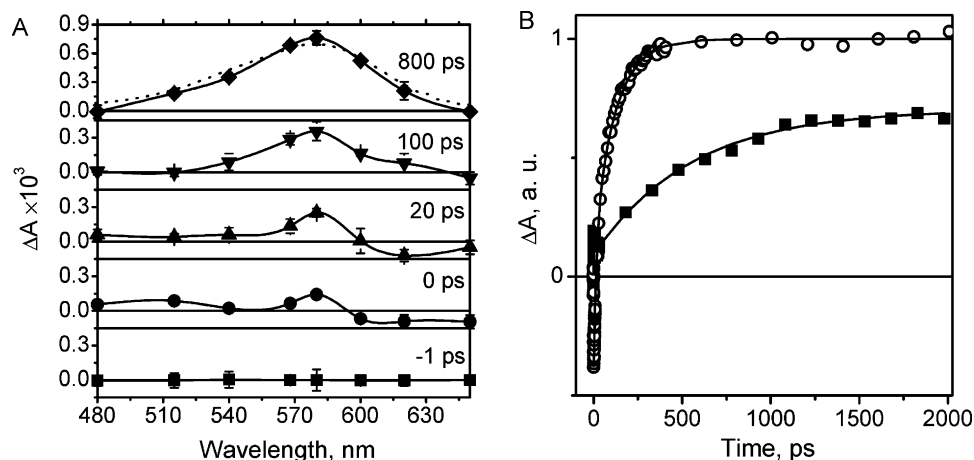


**Figure 1.** (A) SP/DMPC transient absorption difference spectra. Time delays:  $-1$  ps (prior to excitation,  $\blacksquare$ ),  $0$  ps ( $\bullet$ ),  $20$  ps ( $\blacktriangle$ ),  $100$  ps ( $\blacktriangledown$ ), and  $800$  ps ( $\blacklozenge$ ). Error bars are indicated in the spectra. The dotted line ( $\cdots$ ) shows the MC absorption spectrum in toluene solution. (B) Transient absorption kinetics measured at  $568$  nm for SP/DMPC liposomes ( $\blacksquare$ ) and for SP in toluene solution ( $\circ$ ). Fits to the data at  $t > 10$  ps are also shown; rate constants are  $k = (4.8 \pm 0.2) \times 10^9 \text{ s}^{-1}$  for SP/DMPC and  $k = (8.3 \pm 0.2) \times 10^9 \text{ s}^{-1}$  for SP in toluene. Excitation was at  $325$  nm with  $100$  fs pulses, temperature  $25^\circ\text{C}$ .

in toluene solution (see dotted line in Figure 1A). As merocyanines have large solvatochromic shifts (MC absorption maximum shifts from  $585$  to  $525$  nm depending on solvent polarity), similarities in the absorption spectra indicate that the polarity of the MC molecular environment in the bilayer is essentially the same as that in the toluene solution. Therefore, the sensitizers are embedded in the aliphatic interior of the phospholipid bilayer where the effective dielectric permittivity is  $\epsilon \sim 2$ .<sup>27,28</sup> (The polarity of the phospholipid bilayer varies from  $\epsilon \approx 2$  in the aliphatic interior to  $\epsilon = 81$  for the free water).<sup>27,28</sup>

The MC  $\lambda_{\text{max}} = 580$  nm absorption peak does not shift on the  $3$  ns time scale investigated in our transient absorption experiments. On a much slower time scale ( $\gg 3$  ns) the MC absorption maximum in DMPC bilayers shifts to  $\lambda_{\text{max}} = 520$  nm. MC has a much larger dipole moment ( $17.7$  D was determined for a related 6-nitroBIPS spiropyran) than the closed-form SP ( $4.3$  D for 6-nitroBIPS).<sup>29</sup> Thus, this solvatochromic shift is assigned to MC diffusion from the aliphatic bilayer interior to the more polar phosphate headgroup region. Spirooxazine-derived merocyanine diffusion in phospholipid bilayers has been investigated.<sup>28</sup>

Transient absorption kinetics measured in DMPC bilayers and in toluene solution using a  $568$  nm probe wavelength are shown in Figure 1B. (Within the signal-to-noise ratio for the experiment,  $580$  and  $568$  nm kinetics were determined to have identical rise times. A probe wavelength of  $568$  nm was used in temperature dependence studies to avoid stimulated emission contributions to the measured signal). Although the polarity of the bilayer interior is similar to that of toluene (solvatochromic  $\lambda_{\text{max}}$  values are the same), the more viscous environment present in phospholipid bilayers leads to slower isomerization. In bilayers at  $>10$  ps time delay, the kinetics can be described with a single-exponential rise term  $B(1 - \exp(-kt))$ , where  $B$  is amplitude,  $t$  is time, and  $k$  is a rate constant. Nonlinear least-squares fitting of the data to this expression yields  $k = (210 \pm 10 \text{ ps})^{-1} = (4.8 \pm 0.2) \times 10^9 \text{ s}^{-1}$ . Rate constant  $k$  is assigned to isomerization leading to product MC formation. Earlier studies of several spiropyrans in organic solvents<sup>4,5,7-9</sup> also found single-exponential isomerization dynamics. These relatively simple isomerization kinetics enable analysis of the rate constant temperature and viscosity dependence and determination of phospholipid bilayer effects on isomerization rates.

**TABLE 1: Phase Transition Temperatures, Merocyanine Absorption Maxima, and Experimental Rate Constants in the Gel- and Liquid-Phase Phosphatidylcholine Bilayers and in Toluene Solution**

|           | $T_{\text{PT}}$<br>( $^\circ\text{C}$ ) | $\lambda_{\text{max}}^a$<br>(nm) | $k^b$<br>( $\times 10^9 \text{ s}^{-1}$ )<br>8 $^\circ\text{C}$ /gel phase | $k^b$<br>( $\times 10^9 \text{ s}^{-1}$ )<br>53 $^\circ\text{C}$ /liquid phase |
|-----------|---|----------------------------------|--|--|
| DMPC 14:0 | 23                                      | 580                              | $3.2 \pm 0.2$  | $9.7 \pm 0.7$  |
| DPPC 16:0 | 42                                      | 580                              | $1.9 \pm 0.3$  | $9.5 \pm 0.9$  |
| DOPC 18:1 | 11                                      | 580                              | $3.8 \pm 0.2$  | $9.4 \pm 0.3$  |
| toluene   |   | 580                              | $7.6 \pm 0.4$  | $11.4 \pm 0.7$   |

<sup>a</sup> Merocyanine  $\lambda_{\text{max}}$   $800$  ps after the excitation with  $100$  fs pulses at  $325$  nm. <sup>b</sup> Obtained from single-exponential fits to  $568$  nm kinetics at  $10$ – $2000$  ps time delay.

**Isomerization in Liquid- and Gel-Phase Phosphatidylcholine Bilayers.** SP  $\rightarrow$  MC reaction dynamics were investigated in the gel and liquid phases of three common phosphatidylcholines. Table 1 lists lipid phase transition temperatures and MC absorption maxima  $800$  ps after the excitation. The phospholipids in Table 1 have identical choline headgroups ( $-\text{CH}_2\text{CH}_2\text{N}(\text{CH}_3)_3^+$ , Scheme 1) but differ in the length of the fatty acid chains: 14 carbon atoms for DMPC, 16 for DPPC, and 18 for DOPC. (DOPC lipids also have an unsaturated C=C bond at the 9 position, which lowers the phase transition temperature,  $T_{\text{PT}}$ , to  $11^\circ\text{C}$ .) For all phosphatidylcholine bilayers,  $800$  ps transient absorption difference spectra are similar to the steady-state spectrum in toluene. In both gel ( $8^\circ\text{C}$ ) and liquid ( $53^\circ\text{C}$ ) phases, isomerization kinetics (and experimental rate constants  $k$ ) did not differ significantly between DOPC, DMPC, and DPPC lipids (Table 1). For example, in liquid-phase bilayers at  $53^\circ\text{C}$ , isomerization rate constants were in the range  $(9.4\text{--}9.7) \times 10^9 \text{ s}^{-1}$ . In contrast, differences between the gel- and liquid-phase data are important.

**Isomerization Rate Constant Temperature Dependence.** Temperature dependence studies were carried out on SP/DMPC bilayers between  $8$  and  $53^\circ\text{C}$ . This temperature range spans the  $\text{P}_{\beta'} \leftrightarrow \text{L}_{\alpha}$  phase transition for DMPC lipids. (Because of the results shown in Table 1, we expect that the conclusions are also applicable to other phosphatidylcholines.) The isomerization kinetics at all temperatures were single-exponential, but the rate constant  $k$  increased from  $(3.2 \pm 0.2) \times 10^9 \text{ s}^{-1}$  at  $8^\circ\text{C}$  to  $(9.7 \pm 0.7) \times 10^9 \text{ s}^{-1}$  at  $53^\circ\text{C}$ . The transient absorption signal amplitudes at  $1500$ – $3000$  ps time delay were similar at

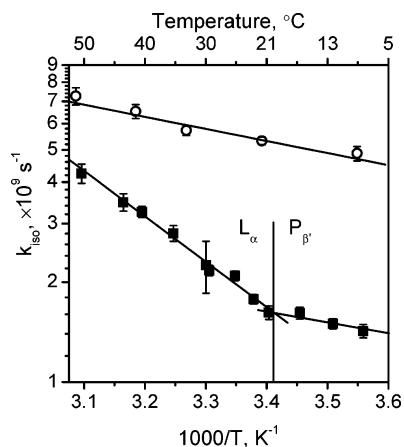


**Figure 2.** Temperature dependence of isomerization rate constants in DMPC bilayers (■) and in toluene solution (○). The  $P_{\beta'} \leftrightarrow L_{\alpha}$  phase transition temperature is indicated in the graph.

all temperatures, suggesting that the quantum yield for the reaction,  $\Phi$ , did not change in this temperature range.

The model of Scheme 1 was used to determine isomerization rate constants,  $k_{\text{iso}}$ , from the experimental data. To describe the photochemical processes in Scheme 1, a system of four first-order differential equations is required.<sup>30</sup> Such a system could only be solved numerically.<sup>30</sup> The analysis can be simplified because  $k_1 \gg k_{\text{iso}}$  for spiropyran compounds.<sup>4,5,7–9</sup> Therefore, very fast formation of intermediate X is followed by slower isomerization ( $k_{\text{iso}}$ ) and ring-closing ( $k_2$ ) processes. Differential equations describing the time-dependent concentrations of intermediate  $[X](t)$  and product  $[MC](t)$  are

$$\frac{d[X](t)}{dt} = -(k_{\text{iso}} + k_2)[X](t) \quad (1)$$

$$\frac{d[MC](t)}{dt} = k_{\text{iso}}[X](t) = k_{\text{iso}}[X_0] \exp(-(k_{\text{iso}} + k_2)t) \quad (2)$$

(Formation of  $[X](t)$  is not included in the model but is described using  $[X_0]$ , the concentration of the intermediate formed after excitation.) The solution of eq 2 is

$$[MC](t) = \frac{k_{\text{iso}}[X_0]}{k_{\text{iso}} + k_2} (1 - \exp(-(k_{\text{iso}} + k_2)t)) = \Phi[X_0] \left( 1 - \exp\left(-\frac{k_{\text{iso}}}{\Phi}t\right) \right) \quad (3)$$

where  $\Phi$  is the quantum yield of the reaction,  $\Phi = k_{\text{iso}}/(k_{\text{iso}} + k_2)$ . Equation 3 represents experimentally measured  $[MC](t)$  concentration time dependence. Therefore, the experimentally measured rate constant,  $k$ , is equal to  $k = k_{\text{iso}}/\Phi$ , and the isomerization rate constant,  $k_{\text{iso}}$ , is

$$k_{\text{iso}} = k\Phi \quad (4)$$

The quantum yield for the reaction,  $\Phi$ , was determined from comparison of MC transient absorption amplitudes in toluene and in DMPC bilayers ( $\Phi = 0.64$  in toluene solution was reported for a related 6-nitroBIPS spiropyran, which was used as a reference).<sup>31</sup> In DMPC liposomes, we found  $\Phi = 0.44$ . The  $k_{\text{iso}}$  temperature dependence calculated according to eq 4 is shown in Figure 2.

As the polarity of the SP membrane environment is similar to that of toluene (solvatochromic  $\lambda_{\text{max}} \approx 580$  nm, Table 1 and Figure 1A), isomerization dynamics in toluene solution were

studied as well. Similar to the results in phospholipid bilayers, 568 nm kinetics in toluene solution could be described by a single-exponential rise with  $k = (7.6 \pm 0.4) \times 10^9 \text{ s}^{-1}$  at 8 °C. At 53 °C, the experimental rate constant increased to  $(11.4 \pm 0.7) \times 10^9 \text{ s}^{-1}$ . Isomerization rate constants in toluene solution (also calculated using eq 4) are contrasted with the results obtained in DMPC liposomes in Figure 2.

As shown in Figure 2,  $k_{\text{iso}}$  data in toluene solution could be described using an Arrhenius expression,  $k = A \exp(-E_a/RT)$ , with an activation energy of  $E_a = 7.1 \pm 0.9 \text{ kJ mol}^{-1}$  and a preexponential factor  $A = (9.8 \pm 0.2) \times 10^{10} \text{ s}^{-1}$ . It is apparent from Figure 2 that the  $k_{\text{iso}}$  temperature dependence in DMPC bilayers differs from that in toluene solution. In particular, a single Arrhenius expression cannot be used to fit SP/DMPC data over the entire temperature range. Instead,  $P_{\beta'}$  and  $L_{\alpha}$  phase data were analyzed independently using two Arrhenius expressions. The Arrhenius preexponential factor,  $A$ , and activation energy,  $E_a$ , changed at  $\sim 20$  °C, which is attributed to the  $P_{\beta'} \leftrightarrow L_{\alpha}$  phase transition ( $T_{\text{PT}} = 23$  °C for DMPC lipids, Table 1). In the  $P_{\beta'}$  phase,  $E_a = 7.3 \pm 1.6 \text{ kJ mol}^{-1}$  and  $A = (3.3 \pm 0.3) \times 10^{10} \text{ s}^{-1}$ . In the  $L_{\alpha}$  phase,  $E_a = 26.0 \pm 1.0 \text{ kJ mol}^{-1}$  and  $A = (6.9 \pm 0.6) \times 10^{13} \text{ s}^{-1}$ . The origin of the reduced activation energy and smaller preexponential factor in the  $P_{\beta'}$  phase is discussed below.

**Intrinsic Barrier for the Isomerization Reaction.** Two effects contribute to the temperature dependence of the isomerization rate constant,  $k_{\text{iso}}$ : the intrinsic barrier for the reaction and molecular friction of the environment.<sup>32–34</sup> These contributions can sometimes be separated using the activated barrier crossing formula, where  $E_{\text{iso}}$  is the intrinsic barrier height,  $R$  is the gas constant, and the reduced rate,  $F(\xi)$ , describes frictional effects<sup>32–34</sup>

$$k_{\text{iso}} = F(\xi) \exp(-E_{\text{iso}}/RT) \quad (5)$$

Molecular activation energy,  $E_{\text{iso}}$ , can be estimated if rate constants are measured in solutions of equal viscosity.<sup>32–34</sup> This is commonly achieved using a homologous series of solvents and adjusting the temperature to obtain isoviscosity conditions.<sup>32–34</sup> We performed such an analysis in *n*-alcohol solutions ( $C_4$ – $C_9$ ) and obtained  $E_{\text{iso}} = 14.2 \pm 0.7 \text{ kJ mol}^{-1}$  (see Supporting Information; alcohol solvents were used to obtain sufficient viscosity variations in the temperature range accessible with a flow cell).  $E_{\text{iso}}$  values found for SP/MC compounds are similar to the isomerization barriers for cyanine dyes and polyenes.<sup>34</sup>

## Discussion

**Isomerization in the Gel Phase of the Bilayer.**  $SP \rightarrow MC$  isomerization in the gel  $P_{\beta'}$  phase is unexpected, as this phase closely resembles a solid-state system.<sup>19</sup> Photochromic reactions have been investigated in the solid state.<sup>35,36</sup> Through the use of spiropyran and spirooxazine microcrystals and amorphous solids, it was shown that the first step of the reaction, breaking of the  $C_{\text{spiro}}-O$  bond, is followed by the reverse reaction without formation of a MC product.<sup>35,36</sup> This was attributed to the small free volume available in the solid state.<sup>35,36</sup> Results are different in phospholipid bilayers, where even in the solid-like  $P_{\beta'}$  phase the  $SP \rightarrow MC$  reaction occurs with a high quantum yield and the isomerization reaction has a lower activation energy than that in the  $L_{\alpha}$  phase (Figure 2).

Formation of the MC product in the gel-phase bilayers could be attributed to the structural heterogeneity of this system. In the  $P_{\beta'}$  phase, the bilayer thickness is about 25% greater than



that in the  $L_\alpha$  phase.<sup>37</sup> This is largely due to the all-trans alkyl chain configuration of the lipids and some separation of the lipid leaflets. In the center of a  $P_\beta'$  phase bilayer (the region of the slip plane between the lipid leaflets), molecular packing is lower than in the fatty acid chain region.<sup>21–25</sup> Spiropyran localization in the middle of the bilayer (between the lipid leaflets) could explain the observed efficient isomerization and reduced activation energy in the  $P_\beta'$  phase. Such a localization would not result in solvatochromic shifts, as the polarity of the central region of the bilayer ( $\sim 20$  Å thickness for DMPC lipids) is approximately constant.<sup>27,28</sup> Localization in the bilayer slip plane may also explain the reduced viscosity dependence (manifesting as a smaller preexponential factor compared to the  $L_\alpha$  phase data). Therefore, detailed analysis of isomerization rate constants in a gel phase requires determination of the molecular geometry (structure) of the spiropyran/bilayer system, which is not presently known.

Observations of facile (high yield and low activation energy) SP/MC isomerization in the gel-phase bilayers support the use of such photochromic reactions to modify phospholipid bilayer properties, including various light-sensitive liposome-based membrane transport<sup>18</sup> and drug delivery<sup>38</sup> systems.

**Analysis of DMPC Bilayer Viscosity Based on MC Isomerization Rates in  $L_\alpha$  Phase Bilayers.** First we consider the possibility of local heating of the bilayer in the course of the photochemical reaction. A liposome with a diameter of 75 nm (determined by dynamic light scattering) contains  $\sim 57\,000$  lipid and  $\sim 1200$  SP molecules (an average DMPC headgroup surface area is  $58.2$  Å<sup>2</sup>;<sup>39</sup> the phospholipid/SP molar ratio is 50:1). The upper limit for the temperature change in the liposome (estimate based on heat capacity  $c_p = 1.65$  kJ mol<sup>-1</sup> K<sup>-1</sup>,<sup>37</sup> sample absorbance of  $\sim 0.3$ , and 325 nm photon energy). Since the MC ground state energy is higher than that of SP<sup>11</sup> and some SP excited-state energy is used in the photochemical reaction, the energy released to the liposome from excited SP molecules will be less than the excitation energy. Therefore, liposome heating is not expected to be significant.

As described in the Results section, the isomerization rate constant,  $k_{\text{iso}}$ , depends on the molecular activation energy,  $E_{\text{iso}}$ , and the viscosity of the medium (eq 5). If we assume that the  $E_{\text{iso}}$  value determined in organic solvents can be used to analyze the data obtained in phospholipid bilayers, then the viscosity-dependent factor  $F(\xi)$  can be determined from eq 5 and the data in Figure 2.

Classical Kramers theory of unimolecular reactions predicts that, subject to strong friction, factor  $F(\xi)$  of eq 5 will vary as  $F(\xi) \propto \xi^{-1}$ , where  $\xi$  is a friction coefficient.<sup>33,34</sup> If the friction in the isomerization reaction arises only from the viscosity of the solvent,  $\eta$ , and Stokes' law ( $\xi = 6\pi r\eta$  for the diffusion of a particle with a radius  $r$ ) applies, then  $F(\eta)$  scales with<sup>33,34</sup>

$$F(\eta) \propto \eta^{-1} \quad (6)$$

Several isomerization reactions show this inverse dependence on the solution viscosity, which is often called the Smoluchowski limit.<sup>33,34,40</sup> If eq 6 applies, then determination of the phospholipid membrane viscosity based on calculated  $F(\eta)$  values is possible. A normalization factor required to use eqs 5 and 6 to estimate bilayer viscosity could be obtained from comparison of isomerization rates in solutions and in bilayers. Similar  $k_{\text{iso}}$  values in DMPC bilayers ( $k_{\text{iso}} = 4.3 \times 10^9$  s<sup>-1</sup> at 53 °C) and in nonanol solution ( $k_{\text{iso}} = 4.0 \times 10^9$  s<sup>-1</sup> at 42 °C and 5 cP) suggest that  $\eta \approx 5$  cP for DMPC at 53 °C. Using these approximations, liquid phase bilayer viscosity can be estimated (Figure 3).

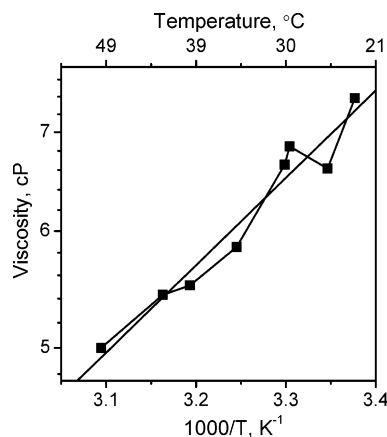


**Figure 3.** DMPC bilayer viscosity temperature dependence determined from  $k_{\text{iso}}$  data in Figure 2, eqs 5 and 6, and assuming  $\eta \approx 5$  cP at 53 °C. Viscosity activation energy is  $E_\eta = 11.3 \pm 1.1$  kJ mol<sup>-1</sup>.

The DMPC bilayer viscosity in Figure 3 appears to have activated temperature dependence. Such an assumption is common in liquid studies and was used for phospholipid bilayers<sup>34,41–43</sup>

$$\eta = \eta_0 \exp(E_\eta/RT) \quad (7)$$

Application of eq 7 to the data in Figure 3 yields  $E_\eta = 11.3 \pm 1.1$  kJ mol<sup>-1</sup> for the  $L_\alpha$  phase DMPC bilayers. The change in  $\eta$  is modest,  $\eta = 7.4$ –5 cP at  $T = 23$ –53 °C. In other studies, much higher  $E_\eta$  values have been found in the  $L_\alpha$  phase bilayers.<sup>41–43</sup> For example,  $E_\eta = 36.0$  kJ mol<sup>-1</sup> has been found in dipyranylpropane excimer formation experiments in DMPC bilayers at  $T = 30$ –60 °C ( $\eta = 22$ –13 cP).<sup>41,42</sup> Likewise, measurements of triplet radical recombination rates in a zinc porphyrin–viologen dyad linked by a  $(\text{CH}_2)_6$  bridge yielded  $E_\eta = 35$  kJ mol<sup>-1</sup> ( $\eta = 80$ –27 cP at 45–70 °C) in the  $L_\alpha$  phase DPPC liposomes.<sup>43</sup>

Possible explanations for the modest viscosity variation and low  $E_\eta$  value in Figure 3 include failure of the Stokes' law and "internal friction" effects (or both). These questions are carefully analyzed for reactions in solution,<sup>33,34</sup> but more work is required to establish the limits of validity of Stokes' law and Kramers theory in phospholipid bilayers. In biophysical cell membrane and phospholipid bilayer studies, Stokes' law is commonly used.<sup>44</sup> For merocyanine 540 excited-state isomerization, rotational diffusion times have been shown to vary linearly with solvent viscosity, indicating that these processes can be described by Stokes' law.<sup>45</sup> Therefore, we assume that the model of eq 6 predicts inaccurate  $E_\eta$  values primarily because of the internal friction effects in our system. In further analysis, we use a modified Kramers model that approximates internal friction with an empirical parameter " $a$ "<sup>33,34</sup>

$$F(\xi) \propto \eta^{-a} \quad 0 < a < 1 \quad (8)$$

The model of eq 8 has been applied to reactions including photochemical ring closure,<sup>46</sup> isomerization of organic molecules,<sup>34</sup> protein folding,<sup>33</sup> and merocyanine decoloration.<sup>47,48</sup> Fractional viscosity dependence has also been studied theoretically. For example, a recent calculation of frequency-dependent friction using a mode coupling theory gives a behavior similar to the power law form.<sup>40</sup>

**Molecular Free Volume in the  $L_\alpha$  Phase DMPC Bilayers.** To apply fractional viscosity dependence model of eq 8 to isomerization in phospholipid bilayers and to determine an

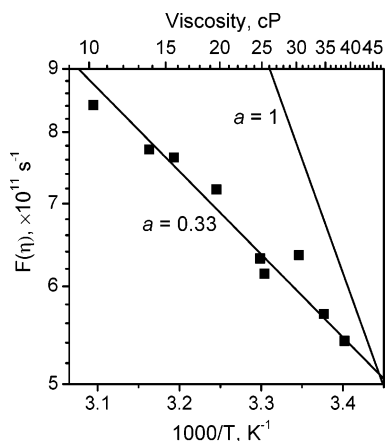


**Figure 4.** Reduced rate  $F(\eta)$  temperature dependence in the  $L_\alpha$  phase DMPC bilayers. The upper axis shows DMPC bilayer viscosity.  $F(\eta)$  values were obtained using eq 5 and  $k_{iso}$  data in Figure 2. Solid lines show  $F(\eta)$  viscosity temperature dependence estimated according to eq 8 with  $a = 0.33$  and  $a = 1$ .

exponent  $a$  value, bilayer viscosity should be determined independently. We use eq 7 and the literature value  $E_\eta = 36$  kJ mol $^{-1}$  for the  $L_\alpha$  phase phosphatidylcholines.<sup>41–43</sup> In this case, bilayer  $\eta$  values range between 40 and 10 cP at 20–50 °C (Figure 4, upper axis). We find that  $a = 0.33 \pm 0.03$  should be used to describe experimental  $F(\eta)$  data in Figure 4 (obtained from Figure 2 using eq 5).

A simple model that accounts for fractional viscosity dependence,  $a < 1$ , is based on comparison of the free volume in the bilayer with the free volume required for isomerization.<sup>49</sup> The free volume required for isomerization consists of two parts: the van der Waals volume occupied by the molecule and additional volume provided by the reaction medium. Therefore, determination of exponent  $a$  in different systems can lead to determination of their free volume properties. Free volume in phospholipid bilayers primarily depends on lipid rotation and alkyl chain isomerization. Because of the ultrafast (picosecond time scale) dynamics considered here, lipid isomerization and rotational motions are essentially frozen. Such conditions are essential for comparison with bilayer simulations carried out on similar time scales.<sup>21–25</sup>

Clustering of the “cavities” between some lipid alkyl chains has been predicted in simulations.<sup>23–25</sup> Such clustering might be necessary for the large-scale isomerization considered here. In the SP  $\rightarrow$  MC isomerization, the substituted benzene moiety moves  $\sim 0.5$  nm, while for a sphere of 0.5 nm radius in the aliphatic bilayer region the available free volume is  $< 1\%$ .<sup>21</sup> Computational studies also predicted that the distribution of “cavities” in the bilayer depends on the lipid structure<sup>23</sup> and on the presence of other membrane components, such as cholesterol.<sup>24,25</sup> Because of the complex depth profile of the bilayer free volume,<sup>21–24</sup> isomerization rates for sensitizers embedded at different depths in the phospholipid bilayers are expected to have different exponent “ $a$ ” values. Different exponent “ $a$ ” values could also be predicted for bilayers composed of several lipids, especially if cholesterol is present<sup>24,25</sup> or lipids have branching fatty acid chains.<sup>23</sup> These predictions remain to be verified experimentally and underscore the importance of studies on well-defined systems. More detailed studies of isomerization reactions in bilayers composed of different lipids that have different free volume distributions<sup>21–25</sup> are required to determine if isomerization rate sensitivity to the bilayer free volume is a general result.

## Summary

Isomerization reactions of photochromic spiropyran/merocyanine compounds were studied in organic solvents and in phosphatidylcholine bilayers. Spiropyran/merocyanine photochromic molecular probes could be used in biophysical membrane studies and provide an interesting system to examine reaction dynamics in a complex environment. We find that isomerization reactions occur in the gel and liquid bilayer phases. Efficient isomerization in the gel phase is unexpected and suggests that spiropyran sensitizers are localized between the lipid leaflets in the gel phase. When the temperature dependence of the isomerization rates in the liquid-phase bilayers are analyzed using a modified Kramers theory, results could be related to the free volume properties of phospholipid bilayers. This suggestion should be tested in further studies.

**Acknowledgment.** This work was supported by Jeffress Memorial Trust and start-up funds from Virginia Commonwealth University.

**Supporting Information Available:** Determination of the intrinsic barrier for the spiropyran isomerization reaction. This material is available free of charge via the Internet at <http://pubs.acs.org>.

## References and Notes

- (1) Korlach, J.; Schwille, P.; Webb, W. W.; Feigenelson, G. W. *Proc. Natl. Acad. Sci. U.S.A.* **1999**, *96*, 8461.
- (2) Mateo, C. R.; Douhal, A. *Proc. Natl. Acad. Sci. U.S.A.* **1998**, *95*, 7245.
- (3) Raymo, F. M.; Giordani, S.; White, A. J. P.; Williams, D. J. *J. Org. Chem.* **2003**, *68*, 4158.
- (4) Ernsting, N. P.; Arthen-Engeland, T. *J. Phys. Chem.* **1991**, *95*, 5502.
- (5) Rini, M.; Holm, A.-K.; Nibbering, E. T. J.; Fidler, H. *J. Am. Chem. Soc.* **2003**, *125*, 3028.
- (6) Tamai, N.; Miyasaka, H. *Chem. Rev.* **2000**, *100*, 1875.
- (7) Zhang, J. Z.; Schwartz, B. J.; King, J. C.; Harris, C. B. *J. Am. Chem. Soc.* **1992**, *114*, 10921.
- (8) Holm, A. K.; Rini, M.; Nibbering, E. T. J.; Fidler, H. *Chem. Phys. Lett.* **2003**, *376*, 214.
- (9) Fidler, H.; Rini, M.; Nibbering, E. T. J. *J. Am. Chem. Soc.* **2004**, *126*, 3789.
- (10) Celani, P.; Bernardi, F.; Olivucci, M.; Robb, M. A. *J. Am. Chem. Soc.* **1997**, *119*, 10815.
- (11) Sheng, Y. H.; Leszczynski, J.; Garcia, A. A.; Rosario, R.; Gust, D.; Springer, J. *J. Phys. Chem. B* **2004**, *108*, 16233.
- (12) Cottone, G.; Noto, R.; La Manna, G. *Chem. Phys. Lett.* **2004**, *388*, 218.
- (13) Futami, Y.; Chin, M. L. S.; Kudoh, S.; Takayanagi, M.; Nakata, M. *Chem. Phys. Lett.* **2003**, *370*, 460.
- (14) Sheng, Y.; Leszczynski, J.; Garcia, A. A.; Rosario, R.; Gust, D.; Springer, J. *J. Phys. Chem. B* **2004**, *108*, 16233.
- (15) Wohl, C. J.; Kuciauskas, D. *J. Phys. Chem. B*, in press.
- (16) Seki, T.; Ichimura, K. *Langmuir* **1988**, *4*, 1068.
- (17) Tanzawa, K.; Hirota, N.; Terazima, M. *Chem. Phys. Lett.* **1997**, *274*, 159.
- (18) Khairutdinov, R. F.; Hurst, J. K. *Langmuir* **2001**, *17*, 6881.
- (19) Yeagle, P. L. *The Membranes of Cells*, 2nd ed.; Academic Press: San Diego, 1993.
- (20) Chiu, D. T.; Wilson, C. F.; Ryttsén, F.; Strömberg, A.; Farre, C.; Karlsson, A.; Nordholm, S.; Gaggari, A.; Modi, B. P.; Moscho, A.; Garza-López, R. A.; Orwar, O.; Zare, R. N. *Science* **1999**, *283*, 1892.
- (21) Marrink, S. J.; Sok, S. M.; Berendsen, H. J. C. *J. Chem. Phys.* **1996**, *104*, 9090.
- (22) Xiang, T.-X. *J. Phys. Chem. B* **1999**, *103*, 385.
- (23) Shinoda, W.; Mikami, M.; Baba, T.; Hato, M. *J. Phys. Chem. B* **2004**, *108*, 9346.
- (24) Falck, E.; Patra, M.; Karttunen, M.; Hyvonen, M. T.; Vattulainen, I. *J. Chem. Phys.* **2004**, *121*, 12676.
- (25) Alinchenko, M. G.; Voloshin, V. P.; Medvedev, N. N.; Mezei, M.; Partay, L.; Jedlovsky, P. *J. Phys. Chem. B* **2005**, *109*, 16490.
- (26) Hobley, J.; Pfeifer-Fukumura, U.; Bletz, M.; Asahi, T.; Masuhara, H.; Fukumura, H. *J. Phys. Chem. A* **2002**, *106*, 2265.
- (27) Stern, H. A.; Feller, S. E. *J. Chem. Phys.* **2003**, *118*, 3401.

- (28) Khairutdinov, R. F.; Giertz, K.; Hurst, J. K.; Voloshina, E. N.; Voloshin, N. A.; Minkin, V. I. *J. Am. Chem. Soc.* **1998**, *120*, 12707.
- (29) Bletz, M.; Pfeifer-Fukumura, U.; Kolb, U.; Baumann, W. *J. Phys. Chem. A* **2002**, *106*, 2232.
- (30) Antipin, S. A.; Petrukhin, A. N.; Gostev, F. E.; Marevtsev, V. S.; Titov, A. A.; Barachevsky, V. A.; Stokach, Y. P.; Sarkisov, O. M. *Chem. Phys. Lett.* **2000**, *331*, 378.
- (31) Horie, K.; Ushiki, H.; Winnink, F. M. *Molecular Photonics: Fundamentals and Practical Aspects*; Wiley-VCH: Weinheim, Germany, 2000.
- (32) Bowman, R. M.; Eisinger, K. B.; Millar, D. P. *J. Chem. Phys.* **1988**, *89*, 762.
- (33) Jas, G. S.; Eaton, W. A.; Hofrichter, J. *J. Phys. Chem. B* **2001**, *105*, 261.
- (34) Waldeck, D. H. The role of solute-solvent friction in large amplitude motions. In *Conformational Analysis of Molecules in Excited States*; Waluck, J., Ed.; Wiley-VCH: New York, 2000; p 113.
- (35) Suzuki, M.; Asahi, T.; Masuhara, H. *Phys. Chem. Chem. Phys.* **2002**, *4*, 185.
- (36) Suzuki, M.; Asahi, T.; Takahashi, K.; Masuhara, H. *Chem. Phys. Lett.* **2003**, *368*, 384.
- (37) Heimburg, T. *Biochim. Biophys. Acta* **1998**, *1415*, 147.
- (38) Guo, X.; Szoka, F. C. *Acc. Chem. Res.* **2003**, *36*, 335.
- (39) Jedlowski, P.; Mezei, M. *J. Phys. Chem. B* **2003**, *107*, 5311.
- (40) Murarka, R. K.; Bhattacharyya, S.; Biswas, R.; Bagchi, B. *J. Chem. Phys.* **1999**, *110*, 7365.
- (41) Zachariasen, K. A.; Kuhnle, W.; Weller, A. *Chem. Phys. Lett.* **1980**, *73*, 6.
- (42) Turley, W. D.; Offen, H. W. *J. Phys. Chem.* **1986**, *90*, 1967.
- (43) Shafirovich, V. Y.; Batova, E. E.; Levin, P. P. *J. Am. Chem. Soc.* **1995**, *117*, 6093.
- (44) Lakowicz, J. R. *Principles of Fluorescence Spectroscopy*, 2nd ed.; Kluwer Academic/Plenum Publishers: New York, 1999.
- (45) Quitevis, E. L.; Horng, M. L. *J. Phys. Chem.* **1990**, *94*, 5684.
- (46) Lipson, M.; Peters, K. S. *J. Phys. Chem. A* **1998**, *102*, 1691.
- (47) Kono, H.; Osako, H.; Sasaki, M.; Takahashi, T.; Ohga, Y.; Asano, T.; Hildebrand, M.; Weinberg, N. N. *Phys. Chem. Chem. Phys.* **2004**, *6*, 2260.
- (48) Volker, E.; O'Connell, M.; Negri, R. M.; Aramendia, P. F. *Helv. Chim. Acta* **2001**, *84*, 2751.
- (49) Gegiou, D.; Muskat, K. A.; Fischer, E. *J. Am. Chem. Soc.* **1968**, *90*, 3907.